Towards the Prediction of Electrochromic Properties of WO3 Films: Combination of Experimental and Machine Learning Approaches

Brandon Faceira, Lionel Teule-Gay, Gian-Marco Rignanese, Aline Rougier

Towards the Prediction of Electrochromic Properties of WO_3 Films: Combination of Experimental and Machine Learning Approaches

Brandon Faceira[1], Lionel Teule-Gay[1], Gian-Marco Rignanese[2], Aline Rougier[1]*
[1]Univ. Bordeaux, CNRS, Bx INP, ICMCB, UMR 5026, F-33600 Pessac, France
[2]UCLouvain, IMCN, Chemin des Étoiles 8, B-1348 Louvain-la-Neuve, Belgium

*corresponding author: aline.rougier@icmcb.cnrs.fr

TOC

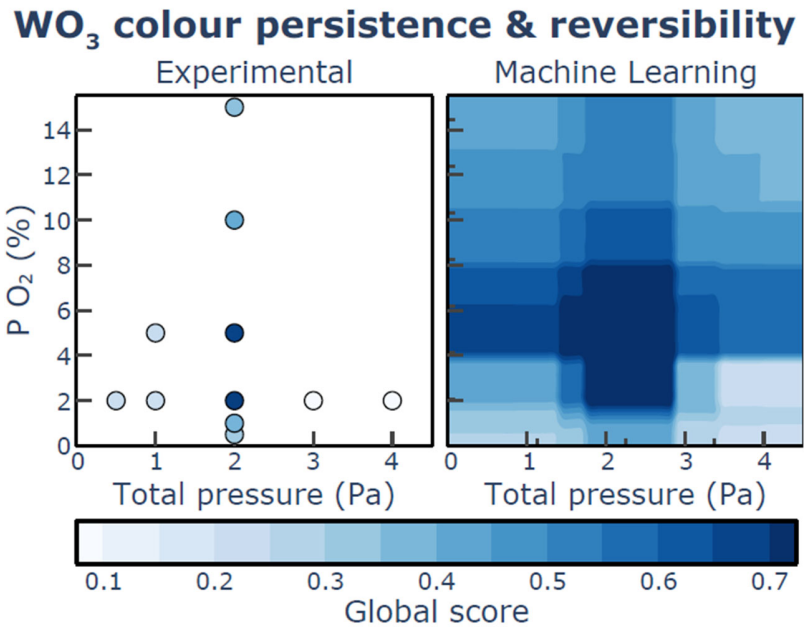

ABSTRACT: WO_3 is the state of the art of electrochromic oxide materials finding technological application in smart windows. In this work, a set of WO_3 thin films were deposited by magnetron sputtering by varying total pressure, oxygen partial pressure and power. On each film two properties were measured, the electrochemical reversibility and the blue colour persistence of Li_xWO_3 films in simulated ambient conditions. With the help of machine learning, prediction maps for such electrochromic properties namely colour persistence and reversibility were designed. High performance WO_3 films were targeted by a global score which is the product of these two properties. The combined approach of experimental measurements and machine learning led to a complete picture of electrochromic properties depending of sputtering parameters providing an efficient tool in regards to time saving.

Global warming and increasing energy demand and consumption urge to search for novel approaches for energy saving. A large part of energy consumption in buildings comes from heating and air conditioning. In order to preserve a comfort while saving energy, smarts windows are a promising solution. Indeed they allow to control incident light radiation in a room while offering outdoor view [1,2]. Smart window technology is often based on electrochromic devices. Electrochromism is the ability of a material to change its optical properties under the appliance of a voltage [3,4]. Among electrochromic materials are found organic molecules, polymers and metal oxides [5]. From this last category, WO_3 is the most studied since the pioneering work of Deb [6]. When elaborated in the form of thin film, WO_3 switches from a colourless state to a dark blue state with the insertion of small cations M (H^+, Li, Na^+) according to $WO_3 + xe^- + xM^+ \Leftrightarrow M_xWO_3$. Electrochromic tungsten oxide films can be amorphous or crystallised depending on the temperature during the elaboration process [7–9]. WO_3 is known to present a self-bleaching behaviour under its reduced state, leading to an increase of the transmittance in open-circuit conditions after the colouration [10,11]. Some authors reported that an additional layer of Ta_2O_5 on top of the WO_3 layer can contribute to increasing the persistence of coloured state of films or based devices once the applied voltage is withdrawn [12,13]. This property is called the memory effect which is defined by the persistence of the coloured (or bleached) state for cathodic (anodic) electrochromic materials under open circuit conditions [14]. Thereby, the applied voltage to obtain the desired state does not need to be applied continuously which leads to increase energy saving of the device. Shi and al. showed that depending on the sputtering conditions leading to different degrees of crystallinity, WO_3 films present a memory effect in air or in an electrolyte media [15].

Generally, aiming to design materials with a desired set of characteristics, experimental research takes a long time to map different process conditions and to characterise them. Moreover,

a limited number of samples can be prepared regarding the time and resources that it takes. In this context of designing properties of materials, machine learning can be a useful tool to help experimentalists [16–18]. This strategy has already been used for the discovery of new compounds in material science [19,20] and in the prediction of material properties [21,22] while scarcely explored in the field of electrochromic materials [23]. The aim of this study is to demonstrate that the traditional experimental approach can be nicely complemented by the use of machine learning algorithms to help find sputtering conditions leading to the desired electrochromic properties: colour persistence (i.e. retention of colour while no potential is applied) as well as good reversibility. Such a combination allows for a significant decrease of the experimental research duration.

WO_3 thin films were elaborated on ITO substrate (commercialized by Solems with a resistance of 30 Ω/□) by Radio Frequency magnetron sputtering at different conditions by varying, RF power, total pressure, oxygen partial pressure and deposition time while keeping a similar film thickness in the range of 210 nm ± 30 nm. Prior to the deposition process, the base pressure in the chamber was set below 3.10^{-5} Pa. Aiming at tuning the memory effect property and in order to map experimental conditions leading to the desired electrochromic properties, a set of WO_3 thin films was prepared by varying sputtering conditions using a WO_3 target of 75 mm of diameter and 3 mm thick (commercialised by Neyco). High reproducibility required a re-oxidation of the target after each deposition performed at 75 W, 5 Pa and 10% O_2 for 1 hour. The initial deposition conditions were a power of 75 W, an oxygen partial pressure of 2 % O_2 and a total pressure of 2 Pa. The Figure 1 shows the cyclic voltammogram of the WO_3 film cycled in a three electrodes cell in a lithium-based electrolyte. The CVs shape is rather typical of amorphous WO_3 with a visual switch from colourless to dark blue colour due to the electrochemical reduction of W^{6+} to W^{5+}.

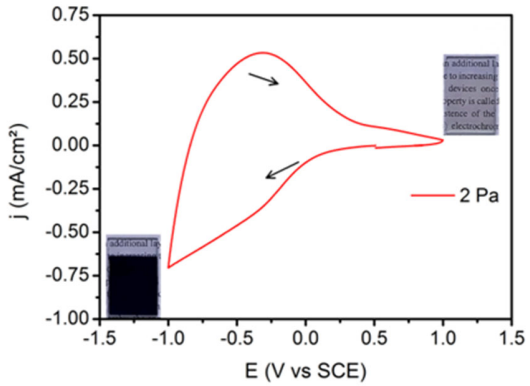

Figure 1. Cyclic voltammogram (1st cycle) of WO_3/LiTFSI in EMIMTFSI (1:9%mol.)/Pt vs SCE cells recorded at 20 $mV.s^{-1}$.

The lithium insertion in WO_3 follows the equation : $WO_3 + xe^- + xLi^+ \Leftrightarrow Li_xWO_3$ (Equation 1), with an amount of inserted lithium about 0.5 estimated during colouration by the equation : $x = \frac{Q.M}{F.p.t}$ where Q (C/cm^2) is the capacity in reduction calculated from $\frac{\int_{-1}^{1} j.dV}{s}$, s is the scan rate (20 $mV.s^{-1}$) , M is the molar mass of WO_3 (231.84 $g.mol^{-1}$), F is the Faraday constant (96 485 $C.mol^{-1}$), p is the density estimated to be 75% of the theoretical WO_3 density (0.75*7.16 g/cm^3) and t is the film thickness.

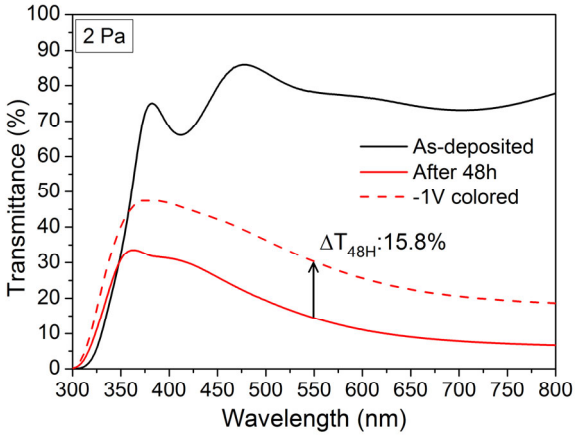

Figure 2. Optical transmittance of $Li_{0.5}WO_3$ before and after 48h at 25 °C and 50 % R.H.

Further cycling protocol consists in 5 CVs in between -1 V and +1 V followed by 5 chronoamperograms, CAs, at +1 V and -1 V for 120 s ended in the blue reduced state. Then *ex-situ* optical measurement was performed on lithiated films just after colouration. In order to evaluate the memory effect of these films, transmission measurements were again recorded after 48 h in a climatic chamber at 25 °C ± 1.3 °C and 50 ± 2.5 % R.H. The optical transmittance of $Li_{0.5}WO_3$ films coloured at -1 V for 120 s and after 48h in the climatic chamber are shown in Figure 2. In air simulated controlled environment, the increase of the transmittance at 550 nm is only of 15.8 % for the WO_3 film deposited at 2 Pa. After 48h, the blue colouration persists indicating that the film presents a memory effect that lasts at least for 2 days.

The mapping was performed by keeping two parameters constant among power, of 50 or 75 W, oxygen partial pressure in the range 0.5 to 15 %, or total pressure in the range 0.5 to 4 Pa, and varying one parameter at the same time. Table 1 gathers the various sets of parameters and corresponding percentages of transmittance modulation, $\Delta T_{48\,h}$ on 12 samples.

Sample	*Total Pressure (Pa)*	*P O_2 (%)*	*Power (W)*	*$\Delta T_{48\,h}$ (%)*	*Persistence score*	*Reversibility score*	*Global score*
1	0.5	2	75	9.8	0.85	0.24	0.20
2	1	2	75	10.5	0.84	0.24	0.20
3	2	2	75	15.8	0.75	0.94	0.71
4	3	2	75	60.4	0.6	0.92	0.05
5	4	2	75	61.1	0.5	0.94	0.05
6	2	0,5	75	43.6	0.32	0.94	0.30
7	2	1	75	38.1	0.41	0.93	0.38
8	2	5	75	15.4	0.76	0.92	0.70
9	2	10	75	32.2	0.50	0.83	0.41
10	2	15	75	35.6	0.45	0.77	0.34
11	2	2	50	64.2	0	0.92	0
12	3	2	50	58.0	0.10	0.93	0.09
13	1	5	75	4.2	0.93	0.23	0.21
14	1	2	50	4.1	0.94	0.31	29

Table 1. Set of experimental data used in the prediction of memory effect property and reversibility of 210 nm WO_3 thin films.

In order to quantify the persistence of the blue colour i.e., the quality of the memory effect, a score using the following somewhat arbitrary formula was adopted:

$$\text{Persistence score} = 1 - \frac{\Delta T_{48h}}{\Delta T_{48h}^{max}} \text{ (Equation 2)}$$

where ΔT_{48h} represents the difference in transmittance at 550 nm between as-coloured films and after 48 h. ΔT_{48h}^{max} is the maximum value of ΔT_{48h} for the set of films. The formula gives a score between 0 and 1, where 0 is the lowest persistence and 1 corresponds to the case where the transmittance at 550 nm is not evolving in 48 h. Based on the data collected for the 12 samples, a machine learning (ML) model was developed for the persistence score as a function of the deposition conditions. The ML model was based on the Random Forest algorithm and the training procedure was repeated 20 times in a bootstrapping approach. The final prediction was taken as the average of the 20 predicted results and their standard deviation provided a measure of the uncertainty. The MAE and RMSE on the persistence score were both smaller than 10%, with a coefficient of determination R^2 of 0.91 (Supporting Information).

Using the ML model, prediction maps for the colour persistence of WO_3 were designed as a function of the sputtering conditions (oxygen partial pressure and total pressure, at fixed power) as reported in Figure 3(a). They can be seen as some form of interpolation of the data listed in Table 1. Adopting an active learning approach, conditions of interest were identified that should lead to higher persistence scores. These are situated around 2 Pa and less. Hence, to obtain high colour persistence in WO_3, the sputtering conditions need to go towards lower total pressure. Two new experimental tests (samples N°13 and 14 in Table 1) were thus conducted adopting a total pressure of 1 Pa. Much higher persistence scores (>0.9) were achieved, confirming the ML predictions.

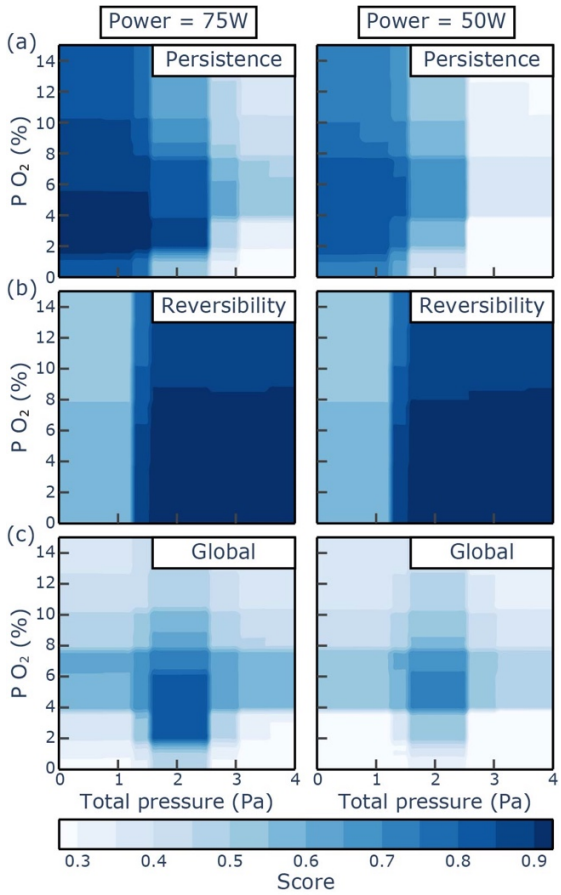

Figure 3. Maps of the (a) persistence, (b) reversibility, and (c) global scores as predicted by the machine learning model trained on the data (samples N°1 to 12) reported in Table 1.

However, for high performance WO_3 films, the colour persistence should be reversible. A reversibility score was thus also introduced. It is calculated based on the first CV cycle as the ratio of electrochemical capacities in oxidation and reduction, $Q_{oxidation}/Q_{reduction}$, as listed in Table 1. Similar to what was done for the persistence score, a ML model was developed for the reversibility score (Supporting Information) and the maps in Figure 3.b) were established. These clearly indicate a poor reversibility for total pressure lower than 2 Pa. In other words, to avoid growing WO_3 films with irreversibility, the choice of the sputtering conditions should tend to high total pressure. From these two maps, colour persistence and reversibility seem to head towards opposite trends. In order to obtain a compromise, a global score was calculated as the product of the persistence and reversibility scores. The corresponding maps are represented in Figure 3.c). It appears that on a tight window around 2 Pa with an oxygen partial pressure between 2% and 6% of sputtering conditions, WO_3 films with a high colour persistence and high reversibility can be prepared. On the basis of these observations, the memory effect property should not correspond only to films with colour persistence but it also needs to present a reversible cycling behaviour.

From Figure 3, fixing the power to 75W and the oxygen partial pressure to 2%, an increase of the total pressure from 1 to 4 Pa should allow one to obtain three kinds of films showing, (i) blue

colour persistence and irreversibility, (ii) high blue colour persistence and reversibility, (iii) limited blue colour persistence and reversibility. Figure 4.a) shows CV of these three kinds of films corresponding to total pressure of 1 Pa, 2 Pa and 4 Pa. At 1 Pa, the CV becomes very flat after the 1st reduction. On the contrary, at 2 and 4 Pa, as predicted the CVs illustrate a nice reversible process. The shift of the oxidation peak towards higher potential at 2 Pa compared to 4 Pa is related to a higher resistance [24,25] as confirmed by the difficulty of the current density to reach 0 mA/cm² at 1 V. On the contrary, for the 4 Pa films, a current density of 0 mA/cm² is reached at 0.75 V. For 2 Pa and 4 Pa, similar x values of Li_xWO_3 around ~ 0.5 are calculated. The poor reversibility of the 1 Pa film indicates that most of the Li^+ and electrons are trapped inside the film through the first cycle and cannot be removed upon further oxidation leading to an irreversible blue colouration.

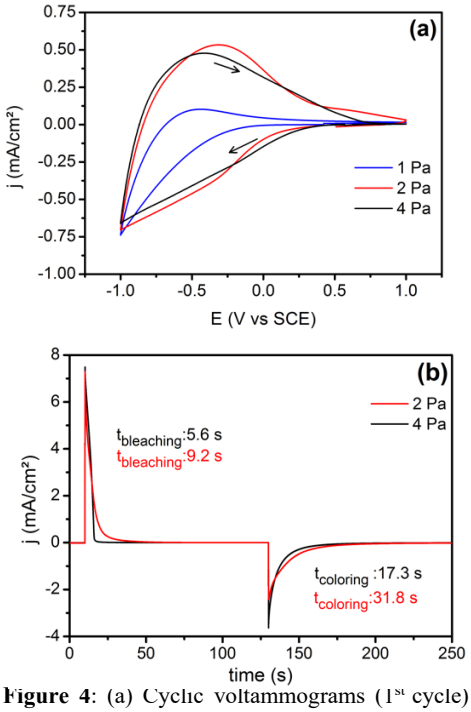

Figure 4: (a) Cyclic voltammograms (1st cycle) for WO_3 thin films deposited at 1 Pa, 2 Pa and 4 Pa in WO_3/LiTFSI in EMIMTFSI (1:9%mol.)/Pt vs SCE cell recorded at 20 mV/s. (b) Chronoamperograms of 2 Pa and 4 Pa during bleaching and colouring under +1V and -1V for 120 s (b).

The reversible character of the films deposited at 2 and 4 Pa is correlated with a switch in colour from colourless to blue (Figure 1). For the 2 Pa, the slower decrease in current density on CVs is associated to higher switching times deduced from chronoamperometry measurements (Figure 4.b). Response time during colouration (reduction) and bleaching (oxidation) correspond to 90 % of current change value as listed in Table 2 [11]. The film deposited at 4 Pa reached faster equilibrium (j = 0 mA/cm²) than the one deposited at 2 Pa. Higher peak current and faster decline indicate a faster electrochemical process [26,27]. In both cases, colouration times are longer than bleaching ones while both are close to twice the ones of 4 Pa for the 2 Pa. This behaviour indicates a higher energy barrier to cross during insertion of lithium. WO_3 is a semi-conducting material, the lithium insertion leads to a more conductive state due to the coexistence of W^{5+} /W^{6+}. The colouring process (Equation 1) starts from a bleached WO_3 state which is more resistive than the lithiated state. Since the resistance of the oxidised state is higher, a much longer process is expected to pass from WO_3 to Li_xWO_3 than the reverse [28,29].

Sample	Colouring time (s)	Bleaching time (s)
2 Pa	31.8	9.2
4 Pa	17.3	5.6

Table 2. Switching times of WO_3 thin films deposited at 2 Pa and 4 Pa.

The origin of the various behaviours lies in the film structure, morphology and composition. Current investigations of the film characteristics are in progress and will be reported in a forthcoming paper.

In summary, combining a machine learning approach to experimental characterisations, based on electrochemical and optical properties, a mapping of the EC performance as memory effect and reversibility of sputtered WO_3 thin films is successfully proposed. Considering the evolution of three main parameters, power, total pressure and oxygen partial pressure, ML leads to a complete picture in which the experimentalists can identify the relevant set of parameters for the desired EC performance. ML provides a significant gain of time. By considering in average 1 film per day, preparing the total grid of oxygen and total pressure requires the production of a least 30 films at one fixed power where 12 films were sufficient in our case with the help of machine learning.

SUPPORTING INFORMATION : The Supporting Information contains detailed information (including the typical errors) about the machine learning models that were developed for the Persistence, Reversibility and Global scores, and about the active learning approach that was used to define the next experimental attempts."

ACKNOWLEDGEMENTS : The authors wish to thank the University of Bordeaux for funding this research and in particular the Ph. D. grant of Brandon Faceira and the invited professor stay of Gian Marco Rignanese. Gian Marco Rignanese is grateful to the F.R.S.-FNRS for financial support

REFERENCES

(1) Granqvist, C. G. Oxide Electrochromics: Why, How, and Whither. *Sol Energy Mater Sol Cells* **2008**, *92* (2), 203–208.
(2) Granqvist, C. G. Electrochromics for Smart Windows: Oxide-Based Thin Films and Devices. *Thin Solid Films* **2014**, *564*, 1–38.
(3) Mortimer, R. J. Electrochromic Materials. *Annu. Rev. Mater. Res.* **2011**, *41* (1), 241–268.
(4) Granqvist, C. G.; Arvizu, M. A.; Bayrak Pehlivan, İ.; Qu, H.-Y.; Wen, R.-T.; Niklasson, G. A. Electrochromic Materials and Devices for Energy Efficiency and Human Comfort in Buildings: A Critical Review. *Electrochim Acta* **2018**, *259*, 1170–1182.
(5) Hassab, S.; Shen, D. E.; Österholm, A. M.; Da Rocha, M.; Song, G.; Alesanco, Y.; Viñuales, A.; Rougier, A.; Reynolds, J. R.; Padilla, J. A New Standard Method to Calculate Electrochromic Switching Time. *Sol Energy Mater Sol Cells* **2018**, *185*, 54–60.

(6) Deb, S. K. Optical and Photoelectric Properties and Colour Centres in Thin Films of Tungsten Oxide. *Philos Mag* **1973**, *27* (4), 801–822.
(7) Bourdin, M.; Mjejri, I.; Rougier, A.; Labrugère, C.; Cardinal, T.; Messaddeq, Y.; Gaudon, M. Nano-Particles (NPs) of WO_3-Type Compounds by Polyol Route with Enhanced Electrochromic Properties. J Alloys Compd **2020**, *823*, 153690.
(8) Li, W.; Zhang, X.; Chen, X.; Zhao, Y.; Sun, W.; Xiao, Y.; Li, S.; Zhao, J.; Li, Y. Long Life All-Solid-State Electrochromic Devices by Annealing. *Sol Energy Mater Sol Cells* **2021**, *224*, 110992.
(9) Rougier, A.; Portemer, F.; Quédé, A.; El Marssi, M. Characterization of Pulsed Laser Deposited WO_3 Thin Films for Electrochromic Devices. Appl Surf Sci **1999**, *153* (1), 1–9.
(10) Kamal, H.; Akl, A. A.; Abdel-Hady, K. Influence of Proton Insertion on the Conductivity, Structural and Optical Properties of Amorphous and Crystalline Electrochromic WO_3 Films. Physica B Condens Matter **2004**, *349* (1–4), 192–205.
(11) Li, X.; Li, Z.; He, W.; Chen, H.; Tang, X.; Chen, Y.; Chen, Y. Enhanced Electrochromic Properties of Nanostructured WO_3 Film by Combination of Chemical and Physical Methods. *Coatings* **2021**, *11* (8), 959.
(12) Nah, Y.-C.; Ahn, K.-S.; Sung, Y.-E. Effects of Tantalum Oxide Films on Stability and Optical Memory in Electrochromic Tungsten Oxide Films. *Solid State Ion* **2003**, *165* (1), 229–233.
(13) Liu, Q.; Dong, G.; Chen, Q.; Guo, J.; Xiao, Y.; Delplancke-Ogletree, M.-P.; Reniers, F.; Diao, X. Charge-Transfer Kinetics and Cyclic Properties of Inorganic All-Solid-State Electrochromic Device with Remarkably Improved Optical Memory. *Sol Energy Mater Sol Cells* **2018**, *174*, 545–553.
(14) Somani, P. R.; Radhakrishnan, S. Electrochromic Materials and Devices: Present and Future. *Materials Chemistry and Physics* **2003**, *77* (1), 117–133.
(15) Shi, Y.; Sun, M.; Zhang, Y.; Cui, J.; Shu, X.; Wang, Y.; Qin, Y.; Liu, J.; Tan, H. H.; Wu, Y. Rational Design of Oxygen Deficiency-Controlled Tungsten Oxide Electrochromic Films with an Exceptional Memory Effect. *ACS Appl. Mater. Interfaces* **2020**, *12* (29), 32658–32665.
(16) Butler, K. T.; Davies, D. W.; Cartwright, H.; Isayev, O.; Walsh, A. Machine Learning for Molecular and Materials Science. *Nature* **2018**, *559* (7715), 547–555.
(17) Schmidt, J.; Marques, M. R. G.; Botti, S.; Marques, M. A. L. Recent Advances and Applications of Machine Learning in Solid-State Materials Science. *npj Comput Mater* **2019**, *5* (1), 83.
(18) Cova, T. F. G. G.; Pais, A. A. C. C. Deep Learning for Deep Chemistry: Optimizing the Prediction of Chemical Patterns. *Front. Chem.* **2019**, *7*, 809.
(19) Oliynyk, A. O.; Antono, E.; Sparks, T. D.; Ghadbeigi, L.; Gaultois, M. W.; Meredig, B.; Mar, A. High-Throughput Machine-Learning-Driven Synthesis of Full-Heusler Compounds. *Chem. Mater.* **2016**, *28* (20), 7324–7331.
(20) Sendek, A. D.; Cubuk, E. D.; Antoniuk, E. R.; Cheon, G.; Cui, Y.; Reed, E. J. Machine Learning-Assisted Discovery of Solid Li-Ion Conducting Materials. *Chem. Mater.* **2019**, *31* (2), 342–352.
(21) Isayev, O.; Oses, C.; Toher, C.; Gossett, E.; Curtarolo, S.; Tropsha, A. Universal Fragment Descriptors for Predicting Properties of Inorganic Crystals. *Nat Commun* **2017**, *8* (1), 15679.
(22) Guo, H.; Zhao, J. Y.; Yin, J. H. Random Forest and Multilayer Perceptron for Predicting the Dielectric Loss of Polyimide Nanocomposite Films. *RSC Adv.* **2017**, *7* (49), 30999–31008.
(23) Gok, E. C.; Yildirim, M. O.; Eren, E.; Oksuz, A. U. Comparison of Machine Learning Models on Performance of Single- and Dual-Type Electrochromic Devices. *ACS Omega* **2020**, *5* (36), 23257–23267.
(24) Al-Shara, N. K.; Sher, F.; Iqbal, S. Z.; Sajid, Z.; Chen, G. Z. Electrochemical Study of Different Membrane Materials for the Fabrication of Stable, Reproducible and Reusable Reference Electrode. *J Energy Chem* **2020**, *49*, 33–41.
(25) Zimmer, A.; Tresse, M.; Stein, N.; Horwat, D.; Boulanger, C. Towards Enhanced Durability of Electrochromic WO_3 Interfaced with Liquid or Ceramic Sodium-Based Electrolytes. *Electrochim Acta* **2020**, *360*, 136931.
(26) Zhang, X.; Dou, S.; Li, W.; Wang, L.; Qu, H.; Chen, X.; Zhang, L.; Zhao, Y.; Zhao, J.; Li, Y. Preparation of Monolayer Hollow Spherical Tungsten Oxide Films with Enhanced near Infrared Electrochromic Performances. *Electrochim Acta* **2019**, *297*, 223–229.
(27) Tong, Z.; Hao, J.; Zhang, K.; Zhao, J.; Su, B.-L.; Li, Y. Improved Electrochromic Performance and Lithium Diffusion Coefficient in Three-Dimensionally Ordered Macroporous V_2O_5 Films. *J. Mater. Chem. C* **2014**, *2* (18), 3651–3658.
(28) Bathe, S. R.; Patil, P. S. WO_3 Thin Films Doped with Ru by Facile Chemical Method with Enhanced Electrochromic Properties for Electrochromic Window Application. Mater Sci Eng B **2020**, *257*, 114542.
(29) Bathe, S. R.; Patil, P. S. Electrochromic Characteristics of Fibrous Reticulated WO_3 Thin Films Prepared by Pulsed Spray Pyrolysis Technique. *Sol Energy Mater Sol Cells* **2007**, *91* (12), 1097–1101.